# Investigating Cooling Load Estimation via Hybrid Models Based on the Radial Basis Function

Sirui Zhang[1], Hao Zheng[2]*
HeBei Petroleum University of Technology, Chengde Hebei, 067000, China

***Abstract*—To advance energy conservation in cooling systems within buildings, a pivotal technology known as cooling load prediction is essential. Traditional industry computational models typically employ forward or inverse modeling techniques, but these methods often demand extensive computational resources and involve lengthy procedures. However, artificial intelligence (AI) surpasses these approaches, with its models exhibiting the capability to autonomously discern intricate patterns, adapt dynamically, and enhance their performance as data volumes increase. AI models excel in forecasting cooling loads, accounting for various factors like weather conditions, building materials, and occupancy. This results in agile and responsive predictions, ultimately leading to heightened energy efficiency. The dataset of this study, which comprised 768 samples, was derived from previous studies. The primary objective of this study is to introduce a novel framework for the prediction of Cooling Load via integrating the Radial Basis Function (RBF) with 2 innovative optimization algorithms, specifically the Dynamic Arithmetic Optimization Algorithm (DAO) and the Golden Eagle Optimization Algorithm (GEO). The predictive outcomes indicate that the RBDA prediction model outperforms RBF in cooling load predictions, with RMSE=0.792, approximately half as much as those of RBF. Furthermore, the RBDA model's performance, especially in the training phase, confirmed the optimal value of $R^2$=0.993.**

***Keywords*—Cooling load estimation; machine learning; building energy consumption; radial basis functions; dynamic arithmetic optimization algorithm; golden eagle optimization algorithm***

## I. Introduction

### A. Background

As building designs become more intricate and demand greater sustainability performance, the utilization of building simulation tools will become unavoidable. Building energy simulation models have undergone over four decades of evolution, with most development endeavors concentrating on refining the model's thermal processes during this time [1]. Four key elements significantly influence a building's energy consumption: (1) its physical attributes, encompassing factors like location, orientation, and type; (2) the installed equipment responsible for maintaining the desired indoor conditions, such as heating, ventilation, air-conditioning systems, electricity, or hot water; (3) external conditions and meteorological variables like temperature, humidity, and solar radiation; and (4) occupant behavior and the associated consequences of their presence [2].

Data on energy consumption across various sectors reveals that the building industry accounts for approximately 40% of the global electricity demand. This electricity is utilized for heating, air conditioning, ventilation, lighting, and the operation of diverse building service systems [3]. For building service systems in tropical or sub-tropical areas, where air conditioning alone accounts for at least 50% of a building's total energy consumption, the proportion is rather higher [4]. However, conducting thorough examinations of energy consumption tends to be expensive and demanding, discouraging property owners and managers from allocating the required investments in terms of time and finances for a comprehensive assessment of energy efficiency. In response to this issue, researchers have developed economical assessment methods designed to identify buildings with potential for energy conservation. The rapid development of building design-specific computer technology and software has made these strategies possible. Computer-based simulation models have been used in many research to evaluate the energy consumption levels of buildings [5]. The most intricate processes within buildings are primarily driven by human behavior, as humans are inherently unpredictable creatures. Human actions significantly impact a building's energy equilibrium, influencing both the indoor environment and the requirements for energy usage [6].

The forward modelling technique is used by several complex computer-based energy simulation programs, such as $\mathrm{DOE-2}$, $\mathrm{EnergyPlus}$, and $\mathrm{BLAST}$. However, developing the simulation model is a very labour- and resource-intensive process, especially for complex mixed-use structures with erratic operating schedules. An alternative method called inverse modelling relies on using current building characteristics, such as energy use, meteorological information, or other relevant performance data, to infer a set of building characteristics, such as cooling loads. Regression analysis has historically been used to use collected data to estimate the distinctive parameters of a structure and its systems. However, the definition of the representative building attributes and the accuracy of the building's performance data sometimes place limitations on the flexibility of inverse models. Obtaining data is another issue that comes up often since it is the foundation for building a working model. In actuality, not every structure that is currently in place has building automation installed. Lack of vital information like as-built building details, system specs, and operating schedules causes several challenges for simulation projects.

## B. Literature Review

AI methods are a viable alternative to traditional approaches, especially in inverse modelling. One such AI tool, known as an artificial neural network(ANN), can effectively approximate nonlinear systems and demonstrate adaptability in complex environments through network training. ANNs, devoid of intricate rules and mathematical procedures, can grasp the intricacies of complex multidimensional systems. Furthermore, ANNs exhibit fault tolerance, robustness, and resilience to noise [7]. Hence, the distinctive attributes of ANN, such as nonlinearity, adaptability, and the capability to map arbitrary functions, render them well-suited for predictive tasks compared to other AI techniques like expert systems, genetic algorithms, and fuzzy logic. ANN is a strong contender for managing building equipment and occupancy data, which inherently contain noise and incomplete information [8], [9], [10], [11], [12], [13], [14]. Furthermore, $ANN$ are widely recognized as a technology that provides an alternative approach to addressing complex and ambiguous problems, primarily due to their robust nonlinear mapping capabilities. Consequently, they have gained significant popularity for use in predicting both building cooling loads [15], [16], [17], [18], [19] and building energy consumption [20], [21], [22].

In energy consumption prediction in building projects, Sapnken et al. [23] conducted a study using data from 7559 buildings and employing nine ML models. Their investigation focused on the efficiency of a Deep Neural Network (DNN) model, demonstrating impressive results and proposing it as an innovative tool for optimizing and predicting energy consumption during the construction design phase of energy-efficient buildings. Leiprecht et al. [24] performed a comprehensive analysis that included autoregressive forecasting methods, decision trees, and "adaptive boosting," exploring deep learning techniques such as Long Short-Term Memory (LSTM) neural networks for thermal load prediction. Jihad and Tahiri [25] utilized ANN to forecast energy requirements in residential structures, achieving satisfactory outcomes with 98.7% accuracy for training data and 97.6% for test data. Wang et al. [26] introduced the Improved Energy Hybrid Optimization (IEHO) neural network, which enhanced the precision of Energy Hybrid Optimization (EHO) approaches. They integrated the Back-Propagation (BP) neural network with the IEHO neural network to form the IEHO-BP neural network model for heating and cooling load forecasting, which demonstrated superior precision. Another study [27] investigated building energy performance using machine learning (ML) techniques including general linear regression, ANNs, decision trees, SVR, and ensemble inference models for cooling and heating load forecasting. This research explored the impact of structural and interior design factors on cooling loads and estimated HVAC system energy demand based on cooling and heating load requirements using various regression models. Cai et al. [28] studied the impact of input factors on heating and cooling loads in residential buildings using the SVR-supervised ML algorithm. They addressed parameter fitting challenges by examining six meta-heuristic optimization algorithms and found that the SVR-AEO hybrid model outperformed others in accurately simulating residential building loads.

Although, several studies have been conducted on the prediction of building loads [29] using ML algorithms [30], also, there are major gaps in the literature in utilizing other algorithms and methodologies such as hybridizing with novel metaheuristic algorithms.

## C. Objectives and Contribution

In the present research, inspiration is drawn from prior successful outcomes that highlighted the superior performance of ANNs compared to other models, leading to the development of Radial Basis Functions (RBF) models for the prediction of cooling loads (CL) in buildings. The contribution of this study lies in exploring novel methodologies to enhance RBF modeling accuracy for CL prediction. The performance of predicting outcomes using a single RBF model was evaluated. To further optimize the training process and improve model performance, two separate optimizers were employed: the DAO and the GEO algorithms. Integrating these optimizers aims to efficiently tune RBF model parameters and enhance predictive accuracy. The novelty of this approach lies in the combination of RBF modeling with advanced optimization techniques, offering a promising avenue to achieve higher accuracy in cooling load prediction. By exploiting the strengths of DAO and GEO, this research extends the boundaries of traditional RBF applications, demonstrating their effectiveness in the context of building energy efficiency studies. The choice of RBF models, coupled with the use of the GEO and the DAO, reflects a strategic approach to enhance the accuracy and efficiency of CL prediction in buildings. RBF models are particularly suitable for nonlinear approximation tasks and offer flexibility in capturing complex relationships within datasets, making them well-suited for CL prediction. The integration of GEO and DAO as optimization techniques is motivated by the need to effectively tune RBF model parameters for optimal performance. GEO, inspired by the behavior of eagles in searching for prey, employs a nature-inspired algorithm to efficiently explore the solution space and converge towards optimal solutions. On the other hand, DAO, characterized by its dynamic arithmetic operations, leverages mathematical principles to guide the optimization process toward improved model fitting.

## D. Research Organization

The introductory part of this study is divided into 4 main sections: background, literature review, objectives, and research organization. Following this, the next section provides detailed explanations about the dataset used and concise descriptions of various ML techniques, including models and optimization algorithms. Section III covers the description of performance evaluators, comparative results using metrics and different techniques, and an analysis comparing the study's findings with existing research. In Section IV, the study's conclusions are summarized.

Fig. 1 shows the process of present study.

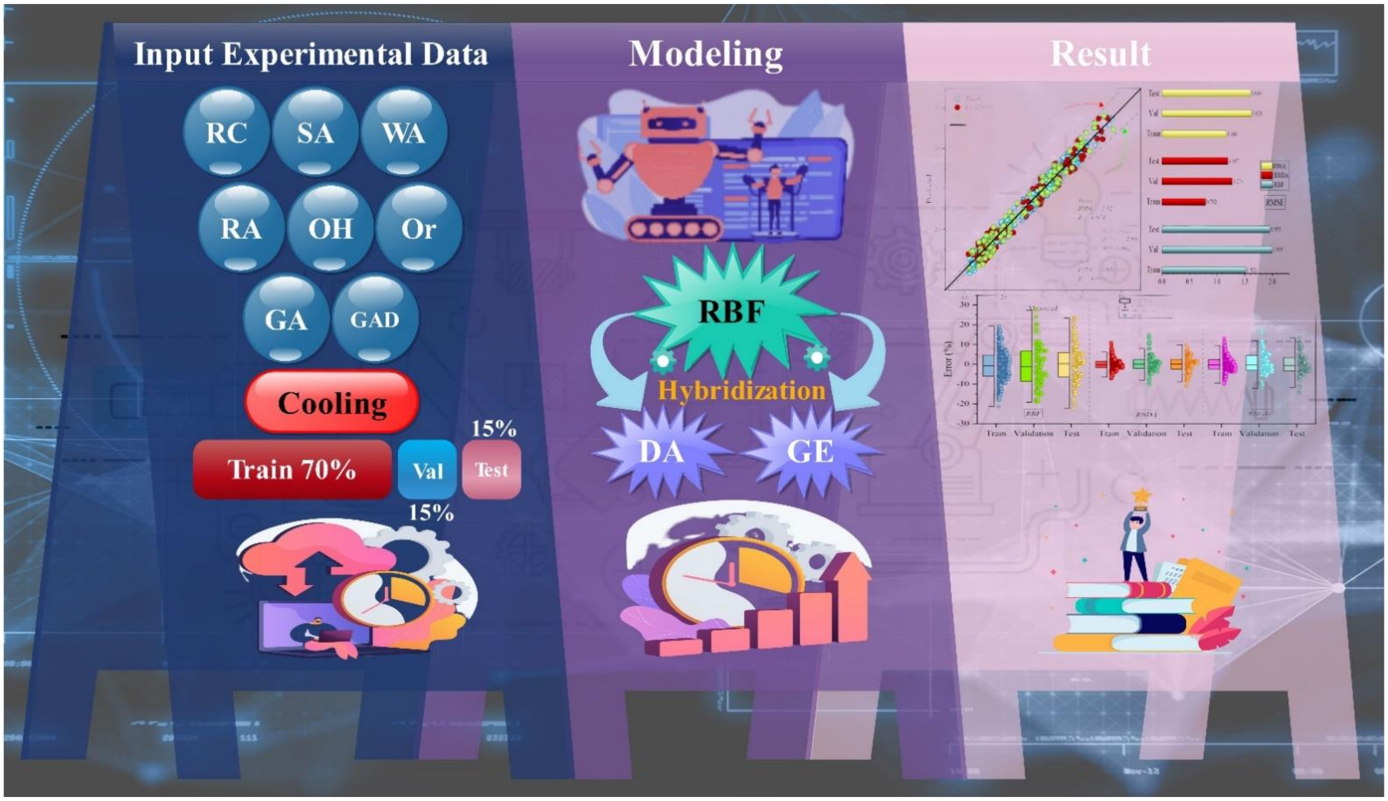

Fig. 1. The current Study's procedure.

## II. Materials and Methods

In the second section of this article, a concise overview of the dataset used in this research is presented, along with descriptions of the ML algorithms selected for implementation in this study, including the RBF model, GEO algorithm, and DAO algorithm. This section provides detailed insights into the dataset characteristics and the rationale behind choosing specific ML techniques to address the research objectives.

### A. Data Collection

The presence of valid and substantial data is paramount in ensuring the credibility and efficacy of the methods outlined in this paper. This study uses a dataset obtained from previous research endeavors [31], [32] to train intelligent models, which comprised 768 data samples. This dataset furnishes essential information required to implement the proposed techniques and assess their performance in predicting building cooling loads. This study's examination of input parameters is predicated on eight important elements, namely relative compactness (RC), surface area (SA), wall area (WA), roof area (RA), orientation (Or), overall height (OH), glazing area (GA), and the distribution of glazing area (GAD). These factors collectively serve as the basis for evaluating and optimizing the predictive models used in this study. Table I details the primary criteria employed for statistically examining the dataset, including metrics such as data averages, standard deviations, and minimum and maximum values. The dataset is partitioned into 70% for training, 15% for validation, and 15% for testing.

TABLE I. The Input Variable's Statistical Characteristics for Cooling

| Variables | | Indicators | | | |
|---|---|---|---|---|---|
| | *Category* | *Min* | *Max* | *Avg* | *St.Dev.* |
| RC | *Input* | 0.62 | 0.98 | 0.764 | 0.106 |
| SA (m2) | *Input* | 514.5 | 808.5 | 671.70 | 88.086 |
| WA (m2) | *Input* | 245 | 416.5 | 318.5 | 43.63 |
| RA (m) | *Input* | 110.25 | 220.5 | 176.60 | 45.165 |
| OH (m) | *Input* | 3.5 | 7 | 5.25 | 1.751 |
| Or | *Input* | 2 | 5 | 3.5 | 1.118 |
| GA (%) | *Input* | 0 | 0.4 | 0.235 | 0.133 |
| GAD | *Input* | 0 | 5 | 2.81 | 1.55 |
| Cooling (kW) | *Output* | 10.9 | 48.03 | 24.587 | 9.51 |

### B. *Overview of ML Method and Optimizers*

*1) Radial Basis Function (RBF):* The Radial Basis Function (RBF) network, a member of the ANNs family, utilizes data-driven methods to establish connections between input and output elements. Instead of relying on mathematical equations, it derives the model's structure and unknown parameters from the provided data [33]. The RBF network is structured into three layers: the input, linear output, and hidden layers. As input vectors traverse the hidden layer, they experience a transformation process, generating radial basis functions.

These operations are executed through an activation process derived from a Gaussian distribution, firmly grounded in the fundamental principles of the Gaussian function. According to the literature, the Gaussian elementary operation ($F_j$) is described as being defined by two critical parameters: width and center [34]. The function is represented in the following manner:

$$F_j(x) = exp\left(\frac{\left|x-\beta_j\right|^2}{2\alpha_j^2}\right) \qquad (1)$$

The output neuron is commonly denoted as:

$$y(x) = \sum_{j=1}^{n} \sigma_j F_j(x) + a \qquad (2)$$

In the above context, $x$ refers to the inputs, $\beta_j$ and $\alpha_j$ reflect the width and center of the Gaussian basis function, individually. And $n$ denotes the number of hidden neurons, $a$ indicates the bias coefficient, and the weight factor that connects the $jth$ hidden neuron to the output neuron is represented by $\sigma_j$.

*2) Dynamic Arithmetic Optimization Algorithm (DAOA):* Adding 2 new accelerator functions has improved the foundational arithmetic optimization algorithm. These modifications affect candidate solutions and the search process, balancing exploration and exploitation dynamically. Unlike other advanced metaheuristics, DAOA stands out because it doesn't need initial parameter adjustments. The DAOA pseudo-code is in Algorithm 1, and the next section explains its dynamic features in detail [35].

ALGORITHM I. PSEUDO-CODE OF *DAOA*

```
procedure Dynamic Arithmetic Optimization Algorithm
Initialize the Algorithm's Parameters $\gamma$; $\mu$
Produce random values to serve as initial positions.
  while ($t <$ maximum number of iterations) Do
                    Evaluate the fitness of given solutions by computing their respective values.
Identify the optimal solution.
Update the DAF value using Eq. (3)
Update the DCS value using Eq. (6)
    for i D 1: number of solutions Do
    for j D 1: number of positions Do
Generate random values in the range of 0 to 1 for r1; r2; r3
    if r1 > DAF then exploration phase
    if r2 > 0:5 then update the solutions' positions
Using first rule in Eq. (4)
      else
Using second rule in Eq. (14)
     end if
   if r1 < DAF then exploitation phase
   if r3 > 0:5 then update the solutions' positions
Using first rule in Eq. (5)
else
Using second rule in Eq. (5)
          end if
        end if
     end for
end for
t D t C 1
end while
Provide the top − performing solution.
  end procedure
```

*a) DAOA's Dynamic accelerated function:* The dynamic aspect of the arithmetic optimization algorithm heavily depends on the Dynamic Accelerated Function (DAF) during the search. It is necessary to adjust the starting values of the accelerated function (Min and Max) in the AOA. However, when a new descending function replaces DAF, it is more desirable to use an algorithm without internally configurable parameters. The adjustment factor for this optimization approach is shown as follows:

$$DAF = (\frac{Iter_{max}}{Iter})^{\gamma} \qquad (3)$$

Here, "$Iter$" reflects the ongoing iteration count, "$Itermax$" is indicated as the upper limit for iterations, and the value of "α" remains a constant. The function experiences a decrease with each consecutive iteration within the algorithm.

*b) Dynamic $DAOA$ candidate solution:* The dynamic properties of $DAOA$ candidate solutions are introduced in this section. The exploration and exploitation stages of metaheuristic algorithms must be approached in a balanced manner for the algorithm to be successful. Every solution in this dynamic adaptation, which prioritizes better exploration and exploitation, iteratively improves its locations by making reference to the optimal solution found during optimization. Eq. (4) in the basic version is replaced by Eq. (5) as a consequence of the inclusion of the Dynamic Candidate Solution ($DCS$) function.

$$x_{i,j}(C_{iter}+1) = \begin{cases} best(x_j) \div (DCS+\epsilon) \times ((UB_j - LB_j) \times \mu + LB_j)) & , \quad r2 < 0.5 \\ best\ (x_j) \times DCS \times ((UB_j - LB_j) \times \mu + LB_j)) & Otherwise \end{cases} \qquad (4)$$

$$x_{i,j}(C_{iter}+1) = \begin{cases} best\ (x_j) - DCS \times ((UB_j - LB_j) \times \mu + LB_j)) & , \quad r3 < 0.5 \\ best\ (x_j) + DCS \times ((UB_j) \times \mu + LB_j)) & , \ Otherwise \end{cases} \qquad (5)$$

The incorporation of the $DCS$ function is a direct response to the diminishing ratio of candidate solutions. Its value consistently diminishes in each iteration, following this established pattern.

$$DCS(0) = 1 - \sqrt{\frac{Iter}{Iter_{max}}} \qquad (6)$$

$$DCS(t+1) = DCS(t) \times 0.99 \qquad (7)$$

Extensive testing involving various hunt agents and iterations has shown that including candidate solutions in $DAOA$ notably speeds up AOA's convergence rate, ultimately improving solution quality. The lack of parameters is often an advantageous feature in metaheuristic algorithms. What sets DAOA apart from AOA is its integration of dynamic functions, while the other aspects of the approach align with the AOA algorithm discussed earlier.

Adaptive parameters help the $DAOA$ algorithm; just the population size and maximum number of iterations need to be adjusted. This algorithm sets itself apart unlike other algorithms that demand problem-specific parameter adjustments. However, it has a drawback: it relies on the iteration count, rather than fitness improvements, as the basis for its adaptive mechanism.

*3) Golden Eagle Optimization (GEO):* This study introduces an innovative swarm-intelligence metaheuristic algorithm inspired by the hunting behavior of golden eagles, referred to as the $GEO$. $GEO$ is rooted in the intelligent adaptation of attack and cruising behaviors observed in golden eagles during their prey search and hunting activities.

The key attributes of the hunting behavior exhibited by golden eagles can be summed up in this way [36]:

They move in a curved trajectory while searching and move in a straight line when attacking.

They tend to start off cruising around when they start hunting and then gradually start to attack more towards the end.

Throughout their flight, they maintain a propensity for both cruising and attacking at all times.

They seek information about prey from other eagles.

The golden eagle's ability to maneuver between flying and hunting is a natural means of exploration, advantage-taking, and transitioning from one to the other. This clears the path for creating a new type of algorithm. The next part shows this behavior mathematically modeled.

*a) Algorithm for optimization and mathematical model:* This section explains how a mathematical equation was created to simulate golden eagle hunting behavior. It introduces the spiral motion formula and then dissects it into attack and cruise vectors, emphasizing the aspects of exploration and exploitation, respectively.

- Golden eagles spiraling around in circles: $GEO$ concentrates on the spiral motion of golden eagles. Every time, golden eagle $'n'$ selects a randomly selected prey from the golden eagle $'f'$ and circles around the ideal spot that the eagle frequents. $'f'$ is designated as a member of the set $\{1,2,\dots,PopSize\}$ because the golden eagle, represented by 'n', has the ability to choose to circle its memory.

- Prey selection: Each iteration involves search agents choosing targets from collective memory. Improved positions replace stored ones. In the GEO approach, golden eagles select prey randomly from any flock member's memory without proximity constraints.

- Attack (exploitation): The attack is a vector from the eagle's current position to its remembered prey. The attack vector for Golden Eagle $n$ can be calculated using Eq. (8).

$$\overrightarrow{A_n} = \overrightarrow{X_f^*} - \overrightarrow{X_n} \qquad (8)$$

Here, $\overrightarrow{X_n}$ is the current position of eagle $n,$ $\overrightarrow{A_n}$ is the eagle's $n$ attack maneuver $and$ $\overrightarrow{X_f^*}$ is the best place (prey) visited so distant by eagle $f$.

- Cruise (exploration): The cruise vector originates from modifying the attack vector. It follows the circle's tangent and stands at a right angle to the attack vector, indicating the eagle's speed concerning the prey. In $i$-dimensional space, it lies within the tangent hyperplane. To determine it, the equation of this hyperplane must be established, involving a point and a perpendicular normal vector. Eq. (9) supplies the scalar representation of this hyperplane in $i$-dimensional space.

$$h_1x_1 + h_2x_2 + h_3x_3 + \cdots + h_ix_i = d \Rightarrow \sum_{j=1}^{i} h_jx_j = d \tag{9}$$

$$\sum_{j=1}^{i} a_jx_j = \sum_{j=1}^{i} a_j^t x_j^* \tag{10}$$

Here ,$\overrightarrow{P} = [p_1, p_2, p_3, \dots, p_i]$ is the hyperplane's arbitrary point and $\overrightarrow{H} = [h_1, h_2, h_3, \dots, h_i\ ]$ is the normal vector, $X = [x_1, x_2, x_3, \dots, x_i]$ is the variables vector, and $d = \overrightarrow{H} \cdot \overrightarrow{P} = \sum_{j=1}^{i} h_j\, p_j . \overrightarrow{X_n}$ (the place of the eagle $n$) is considered as any random location inside the hyperplane and reflect $\overrightarrow{A_n}$ (the point of attack) as the hyperplane may be shown using its normal to which $\vec{C}_n^t$ (The cruise vector in iteration $t$ for the Golden Eagle $n$) belongs version to Eq. (10).

Here, $X^* = [x_1^*, x_2^*, x_3^*, \dots, x_i^*]$ is the chosen prey's location, and $A_n = [a_1, a_2, a_3, \dots, a_i]$ is the attack vector, $X = [x_1, x_2, x_3, \dots, x_i]$ is the decision/design variables vector; it's time to find a cruise vector inside the cruise hyperplane that was calculated for Eagle $n$ in iteration $t$.

The final dimension is determined based on its compatibility with the hyperplane equation, resulting in $i$ — 1 free variable and a single fixed variable. To locate a chance $i$-dimensional objective point $C$ on the golden eagle $n$'s journey hyperplane: Step 1. Arbitrarily pick one variable from the set of $i$ variable stars as the fixed variable, denoting its index as $k$. Notably, avoid selecting a fixed variable among those associated with zero elements in the attack vector $\overrightarrow{A_n}$.

When a variable's coefficient in Eq. (9) is $0$, the line becomes parallel to that variable's axis, allowing it to take any value while the other $i-1$ variables vary randomly. As an instance, in the $3D$ plane $3x_1 + 2x_2 = 10$, if $k = 3$ and random numbers for $x_1$ and $x_2$ is selected, say $\{x_1 = 2, x_2 = 5\}$, a unique point cannot be found. Rather, this plane generates an endless number of points, all of which fulfill the {[2,5,1], [2,5,2], [2,5,3], …} plane equation. Step 2: Give each variable a random value, except for the $k-t$™ variable, which always has the same value. Determine the fixed variable's value in Step 3 by using Eq. (11).

$$c_k = \frac{d - \sum_{j,j\neq k} a_j}{a_k} \tag{11}$$

Here $c_k$ denotes the $k-th$ element of the terminus point $C$, $a_j$ represents the $j-th$ element of the attack vector $A_n$, $d$ refers to the right−hand side of the Eq. (9), $a_k^t$ signifies the $k-th$ element of the attack vector $\overrightarrow{A_n}$, and $k$ shows the directory of the fixed variable. The cruise hyperplane now has a new random destination point. Eq. (12) shows how to find the location of the cruise hyperplane's destination.

$$\vec{C}_n = (c_1 = rand\ , c_2 = rand, \dots, c_k = \frac{d - \sum_{j;j\neq k} a_j}{a_k}\ , \dots, c_i = rand \tag{12}$$

In iteration $t$, the cruise vector for Golden Eagle $n$ may be computed once the destination point has been determined. Random integers between 0 and 1 make up the components of the destination location. The golden eagle population is guided by the cruise vector away from their prior memory, highlighting the discovery phase of $GEO$.

- Transferring to new roles

The golden eagles use both assault and cruise vectors when they travel. According to Eq. (13), the step vector for golden eagle $n$ is described in iteration $t$.

$$\Delta x_n = \vec{r}_1 p_a \frac{\overrightarrow{A_n}}{\|\overrightarrow{A_n}\|} + \vec{r}_2 p_c \frac{\vec{C}_n}{\|\vec{C}_n\|} \tag{13}$$

The coefficients $p_a^t$ and $p_c^t$ in iteration $t$ control the impact of attack and cruise on golden eagles. Random vectors $\vec{r}_1$ and $\vec{r}_2$ have elements within [0,1]. The discussion of $p_a$ and $p_c$ will follow.$\|\vec{C}_n\|$ and $\|\overrightarrow{A_n}\|$ represent the attack and cruise vectors' Euclidean norms, as determined by Eq. (14).

$$\|\overrightarrow{A_n}\| = \sqrt{\sum_{j=1}^{i} a_j^2}\ , \|\vec{C}_n\| = \sqrt{\sum_{j=1}^{i} c_j^2} \tag{14}$$

The step vector from iteration $t$ is added to the locations of the golden eagles in iteration $t$ to calculate their positions in iteration $t + 1$.

$$x^{t+1} = x^t + \Delta x_i^t \tag{15}$$

Golden Eagle $n$ updates its memory if its new position is superior; otherwise, it retains its memory but adopts the new position. In each iteration, eagles pick a random peer to circle the best-visited spot, determining attack and cruise vectors, step size, and the next position. This cycle repeats until one of the termination conditions is satisfied. Eq. (13) involves 2 coefficients, the attack constant $p_a^t$ and cruise constant $p_c^t$, which controls how the step vector is influenced by cruise and attack vectors. The following subsection, denoted as $c$, explains how these coefficient values change throughout the iterations.

- Transition from exploration and exploitation

Golden eagles primarily cruise early in their hunting flight, transitioning to attacking later. These parallels heightened exploration in greater exploitation and initial iterations in later iterations within the future optimizer.

GEO employs $p_a$ and $p_c$ to transition from exploration to exploitation. It begins with a low $p_a$ and high $p_c$ values. As iterations advance, $p_a$ increases gradually, while $p_c$ decreases gradually. Users define the initial and final parameter values, and it is possible to compute intermediate values by using the linear transition described in Eq. (16).

$$\begin{cases} p_a = p_a^0 + \frac{t}{T}\left|p_a^T + p_a^0\right| \\ p_c = p_c^0 + \frac{t}{T}\left|p_c^T + p_c^0\right| \end{cases} \tag{16}$$

In the formula, $t$ represents the current iteration, $T$ is the maximum iteration count, $p_a^0$ and $p_a^T$ stand for the initial and final values of the propensity to attack ($p_a$), respectively, while $p_c^0$ and $p_c^T$ denote the initial and final values of the propensity to cruise ($p_c$), respectively. These tests, which will be covered in more detail later, show that $[p_a^0 and\ p_a^T] = [0.5, 2]\ and\ [p_c^0 and\ p_c^T] = [1, 0.5]$ are suitable parameter settings. This suggests that in the first iteration, $pstarts$ at 0.5 and climbs linearly to reach 2 in the last iteration. In a similar manner, $pc$ starts at 1 in the first iteration and decreases linearly to 0.5 in the last. It's crucial to remember that Eq. (16) uses a linear strategy to change these values; however, logarithmic or other functions might be used as an alternative.

### C. Research Methodology

The research methodology can be delineated in the following manner:

*1) Introduction:* In this study, the consideration of a crucial problem is introduced, with a focus on the imperative for enhanced performance in the RBF model. Significance is placed on the advancement of the field of ML, particularly in practical applications within building energy prediction. The pressing need for improved efficiency in the RBF model is addressed, contributing to the broader landscape of ML and its application to real-world challenges in buildings.

*2) Hybridization method:* A novel ML approach is presented, involving the hybridization of 2 advanced optimization techniques. The combination of optimization methods used to enhance the performance of the RBF model is detailed. Through the strategic integration of these advanced optimization techniques, an innovative perspective is introduced to ML, with a primary goal of elevating the efficiency of the RBF model.

*3) Optimizers used:* In this research, the introduction and detailed description of the 2 distinct optimizers employed in the hybridization method, namely the DAO and the GEO, are provided. The unique strengths of each optimizer and the rationale behind their selection for the hybrid model are thoroughly explained, contributing to a comprehensive understanding of the strategic integration of these optimizers in the research framework.

*4) Model evaluation:* A comprehensive evaluation of both single and hybridized RBF models is undertaken in this study, utilizing established performance metrics such as R$^2$ and RMSE. The choice of these metrics is justified to ensure an impartial assessment of model performance, enhancing the reliability and objectivity of the evaluation process.

*5) Performance comparison:* The performance of hybridized models is compared with the traditional RBF model in this study to emphasize the superiority of the proposed approach. Statistical analyses or visual representations of the results are provided to support the claims made, enhancing the credibility and clarity of the comparison between the 2 model types.

*6) Conclusion:* This section provides a summary of the research's main conclusions and their consequences offering a concise overview of the study's outcomes. Additionally, the limitations of the study are discussed to encourage further exploration in related domains.

## III. Results and Discussion

### A. Prediction Performance Analysis

This research created an ML model called RBF to forecast CL. In addition, the research used two effective optimization algorithms, DAO and GEO, to make hybrid RBF models better at adjusting the settings of the models. The dataset was split into three smaller groups: training, validation, and testing. The training group had 70% of the data, the validation group had 15%, and the testing group had the remaining 15%. The models were evaluated in Table II by comparing different measures, like $R^2$(coefficient of determination), $RMSE$ (Root Mean Square Error), $MAE$ (Mean Relative Absolute Error), NMSE (Normalized Mean Squared Error), and PI (prediction interval). These measures were defined in $Eqs.$ (17) to (21):

$$R^2 = \left(\frac{\sum_{i=1}^{n}(T_i - \bar{T})(P_i - \bar{P})}{\sqrt{\left[\sum_{i=1}^{n}(T_i - \bar{P})^2\right]\left[\sum_{i=1}^{n}(P_i - \bar{P})^2\right]}}\right)^2 \tag{17}$$

$$RMSE = \sqrt{\frac{\sum_{i=1}^{n}(P_i - T_i)^2}{n}} \tag{18}$$

$$MAE = \frac{1}{n}\sum_{i=1}^{n}\|P_i - T_i\| \tag{19}$$

$$NMSE = \frac{\frac{1}{n} \times \sum((y_i - \hat{y}_i)^2)}{\frac{1}{n} \times \sum y_i^2} \tag{20}$$

$$PI = \bar{x}_2 \pm t_{(\alpha/2,\ N-2)} * q^2 \tag{21}$$

Where $n$ is the number of the data points, $T_i$ and $P_i$ are the test and predicted results, respectively. $\bar{P}$ and $\bar{T}$ are the average of the test and prediction result values, $y_i$ represents the actual values, $\hat{y}_i$ denotes the predicted values, $q^2$ signifies the average error value that has been combined from both groups; the t-value corresponding to the desired level of confidence ($\alpha$) and degrees of freedom ($N-2$) is obtained from the $t$ distribution at the critical level of ($\frac{\alpha}{2}, N-2$)."

The following discourse offers a comprehensive analysis of the model's capability to predict CL effectively:

- The RBDA hybrid model showcased exceptional performance, achieving the highest $R^2$ values such as $R^2_{train} = 0.993$, $R^2_{validation} = 0.984$, $R^2_{test} = 0.984$ and $R^2_{all} = 0.990$. The elevated $R^2$ values indicate a robust alignment among the model and the dataset, emphasizing the dependable nature of the selected input variables as strong predictors of the predictable output. Additionally, in the case of both hybrid models, the $R^2$ value during the training phase is higher than in the testing phase. This discrepancy suggests suboptimal training performance in the developed models.
- A Prediction Interval is a statistical metric that quantifies the level of uncertainty associated with a model's predictions. It sets itself apart from a point estimate, such as a mean or median, by defining a range or interval in which future observations are anticipated to occur with a specified confidence level. Among all the models, RBDA stands out with its minimal PI value of 0.019, indicating the lowest degree of uncertainty.
- The RMSE varies across a range, with a minimum of 0.792 (observed during the training phase of RBDA) and a maximum of 1.996 (noted during the RBF single model validation phase). Furthermore, during the training phase of RBDA, the MAE and NMSE values, specifically 0.542 and 0.001, respectively, were observed. This additional evidence solidifies the RBDA hybrid model's high level of accuracy.

TABLE II. THE OUTCOME OF MODELS CREATED FOR RBF

| Model | Phase | Index values | | | | |
|---|---|---|---|---|---|---|
| | | ***RMSE*** | ***R²*** | ***MAE*** | ***NMSE*** | ***PI*** |
| RBF | *Train* | 1.522 | 0.974 | 1.313 | 0.004 | 0.031 |
| | *Validation* | 1.996 | 0.963 | 1.764 | 0.035 | 0.041 |
| | *Test* | 1.956 | 0.961 | 1.667 | 0.033 | 0.040 |
| | *All* | 1.671 | 0.970 | 1.433 | 0.004 | 0.034 |
| RBDA | *Train* | 0.792 | 0.993 | 0.542 | 0.001 | 0.016 |
| | *Validation* | 1.274 | 0.984 | 0.848 | 0.014 | 0.026 |
| | *Test* | 1.197 | 0.984 | 0.836 | 0.013 | 0.024 |
| | *All* | 0.947 | 0.990 | 0.632 | 0.001 | 0.019 |
| RBGE | *Train* | 1.167 | 0.985 | 0.778 | 0.003 | 0.024 |
| | *Validation* | 1.622 | 0.974 | 1.139 | 0.023 | 0.033 |
| | *Test* | 1.603 | 0.972 | 1.062 | 0.022 | 0.033 |
| | *All* | 1.316 | 0.981 | 0.875 | 0.002 | 0.027 |

Fig. 2 illustrates dispersed visualizations of the correlation between predicted and measured CL values. These scattered data points are derived from the 2 evaluation sets based on RMSE and $R^2$. In a broad sense, RMSE serves as a dispersion controller, meaning that lower values of this metric correspond to higher data point density. Moreover, the $R^2$ metric tends to cluster testing and training data points closer to the centerline.

The figure incorporates several additional elements, including a central line at the Y=X coordinates and 2 lines positioned below and above the central line to represent a 10% underestimation and 10% overestimation range. Upon conducting an exhaustive comparison across the three predictive models, it becomes evident that all models exhibit favorable $R^2$ values. This is observed through the proximity of data points associated with these models to the central best-fit line, with most points falling within the boundaries defined by the 2 threshold lines.

Among the 2 optimized RBF models, it is discernible that the data points exhibit greater proximity to the central line, indicating superior performance compared to the single RBF model. In the comparative evaluation of the optimized models, upper and lower threshold lines are employed as reference points. Notably, it becomes evident that the data points about the model optimized through the DAO are consistently contained within the demarcated threshold lines. Conversely, the data points associated with the model optimized through the GEO exhibit a somewhat greater degree of dispersion relative to the prescribed boundaries.

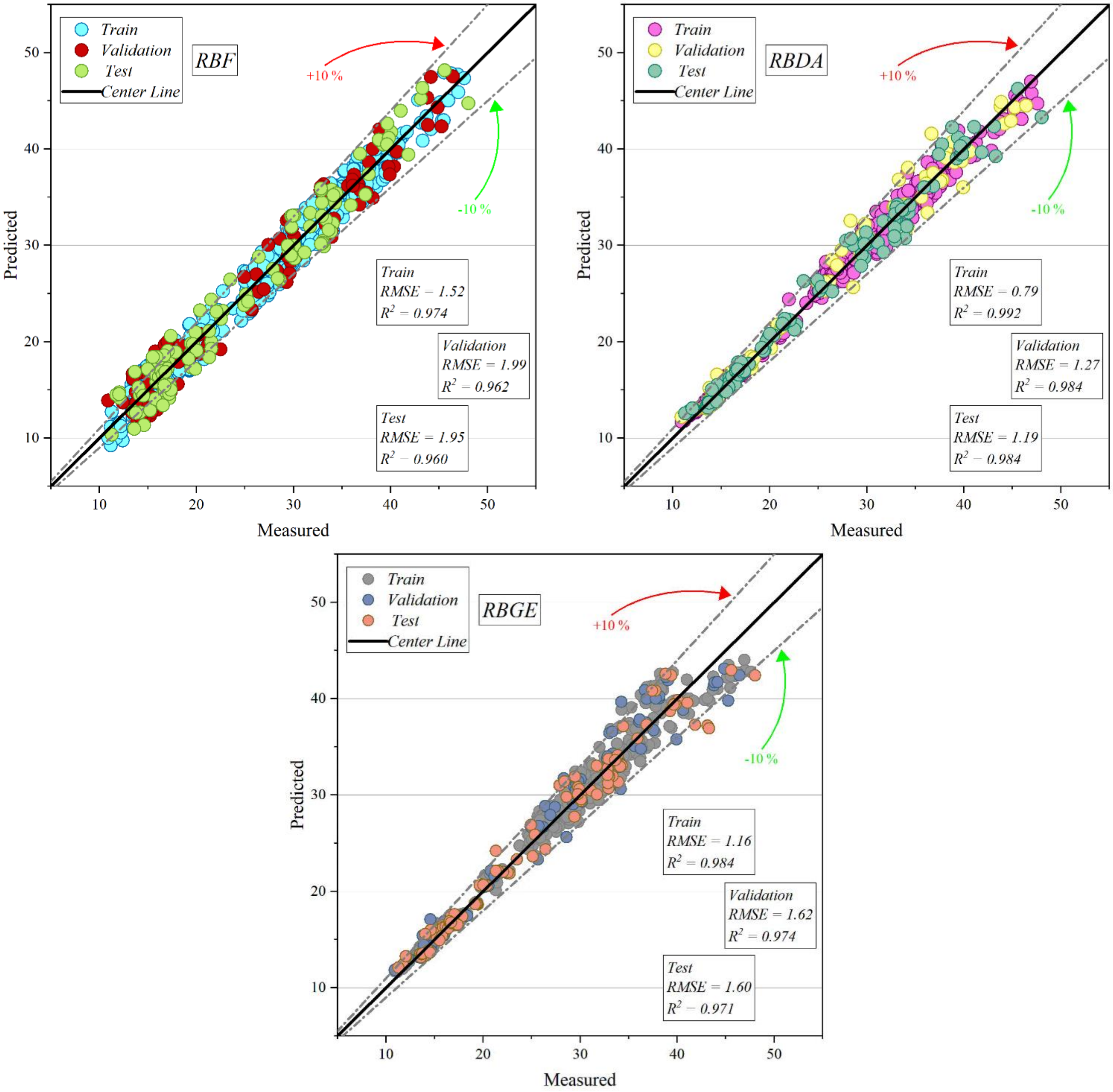

Fig. 2. The scatter plot for developed hybrid models.

This academic research uses a stacked bar plot, as shown in Fig. 3, to compare many parameters in-depth. By stacking the measurements inside of separate bars, this visualization technique offers a succinct and understandable representation of the correlations between various measures. Because each statistic is represented by a different hue, it is easier to see how each one contributes to the final outcomes. The calculated RMSE, $R^2$, and MAE values for the different models are shown in Fig. 3. Upon closer examination, it becomes evident that the RBDA model exhibits lower error rates according to the RMSE = 0.792 and MAE = 0.542 compared to RBF and RBGE. Furthermore, concerning prediction accuracy, as evidenced by the $R^2$ values, it is noteworthy that RBF ($R^2$= 0.974) and RBGE ($R^2$= 0.984) exhibit lower values when compared to the RBDA model.

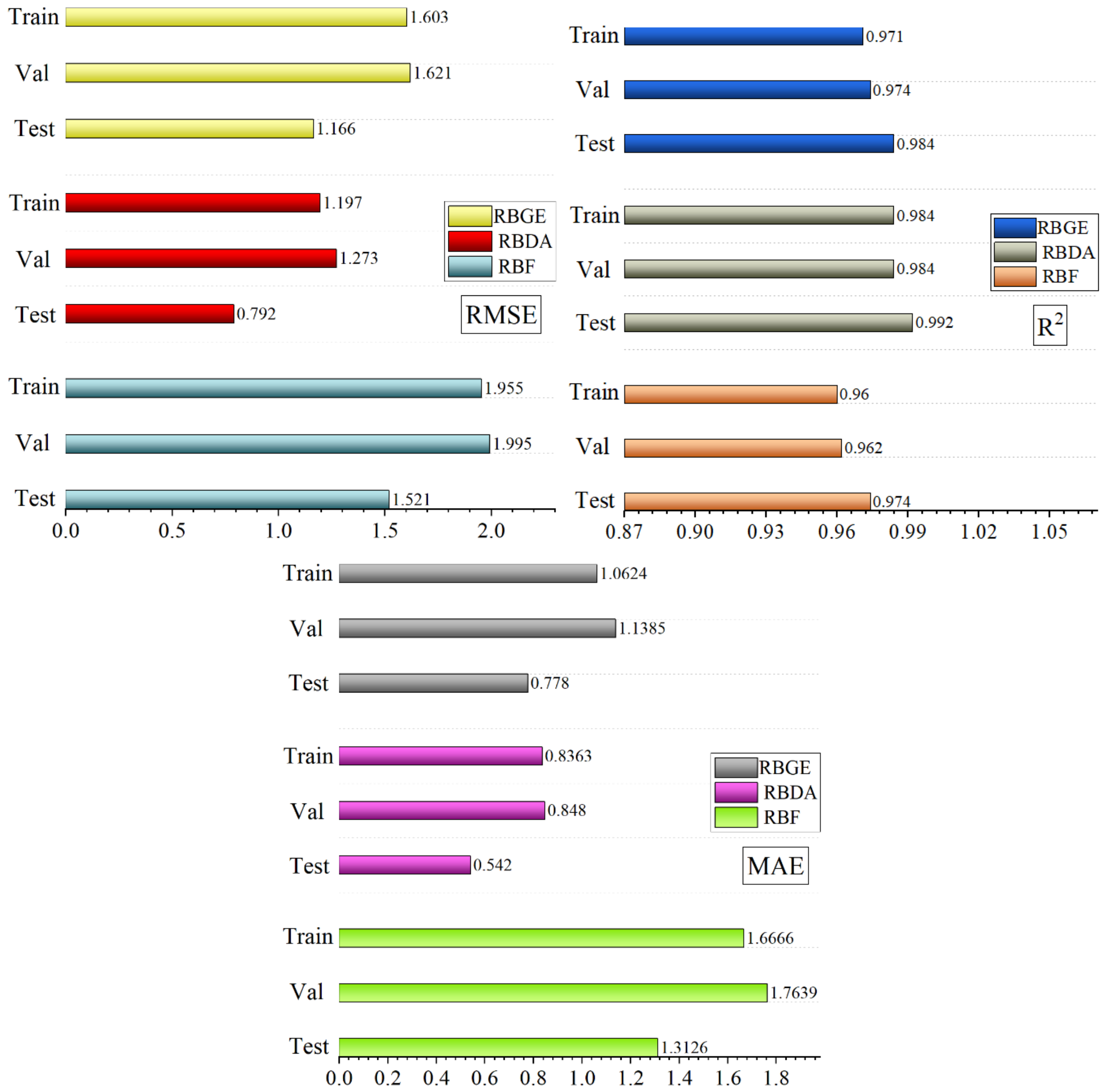

Fig. 3. Comparison between models is based on RMSE, R$^2$, and MAE.

In Fig. 4 and Fig. 5, the error percentages (%) for the models are visualized using both normal distribution plots and the half-boxes, with the errors categorized across the training, validation, and test datasets. As depicted in Fig. 4, the normal distribution plot illustrates that RBDA exhibits a narrow bell-shaped distribution line during the training phase with a higher concentration of errors in the zero percent range, thus indicating its superior performance. However, in the validation and testing phases, the distribution curves for RBF and RBDA resemble each other, whereas RBF shows a wider spread of error values across a broader range. Upon examining the spectrum of error values presented in Fig. 5 for the various models, it becomes evident that the training phase of RBF exhibits the widest range of error values, while the validation phase of RBF displays the narrowest range. Noteworthy is the consistent excellence in performance displayed by the RBDA hybrid model throughout all three phases when considering a range of box proportions related to 25% to 75% of error values. It is essential to underscore that the model's performance exhibits a discernible enhancement as the box proportions approach zero. Moreover, according to RBGE half boxes, it can be observed that it exhibited marginal variation and secured the second position in terms of performance ranking.

## B. Comparing the results of this study and existing studies

Numerous studies have been conducted on CL prediction, including investigations by Afzal et al. [37] using the *MLP* model, and Gong et al. [38] employing the GBM technique. Among the existing publications reported in Table III, superior performance was demonstrated by the GPR model, achieving an R$^2$ value of 0.99 and an RMSE value of 0.059 in a study showed by Roy et al. [39]. A fundamental framework based on the RBF model was used in the present research, and it was improved by hybridizing it with the GEO and DAO algorithms. After analyzing the data, it was discovered that the TDO integration into the RFR model had remarkable applicability. It outperformed the other models in this research, with an R$^2$ value of 0.997 and an *RMSE* of 0.498.

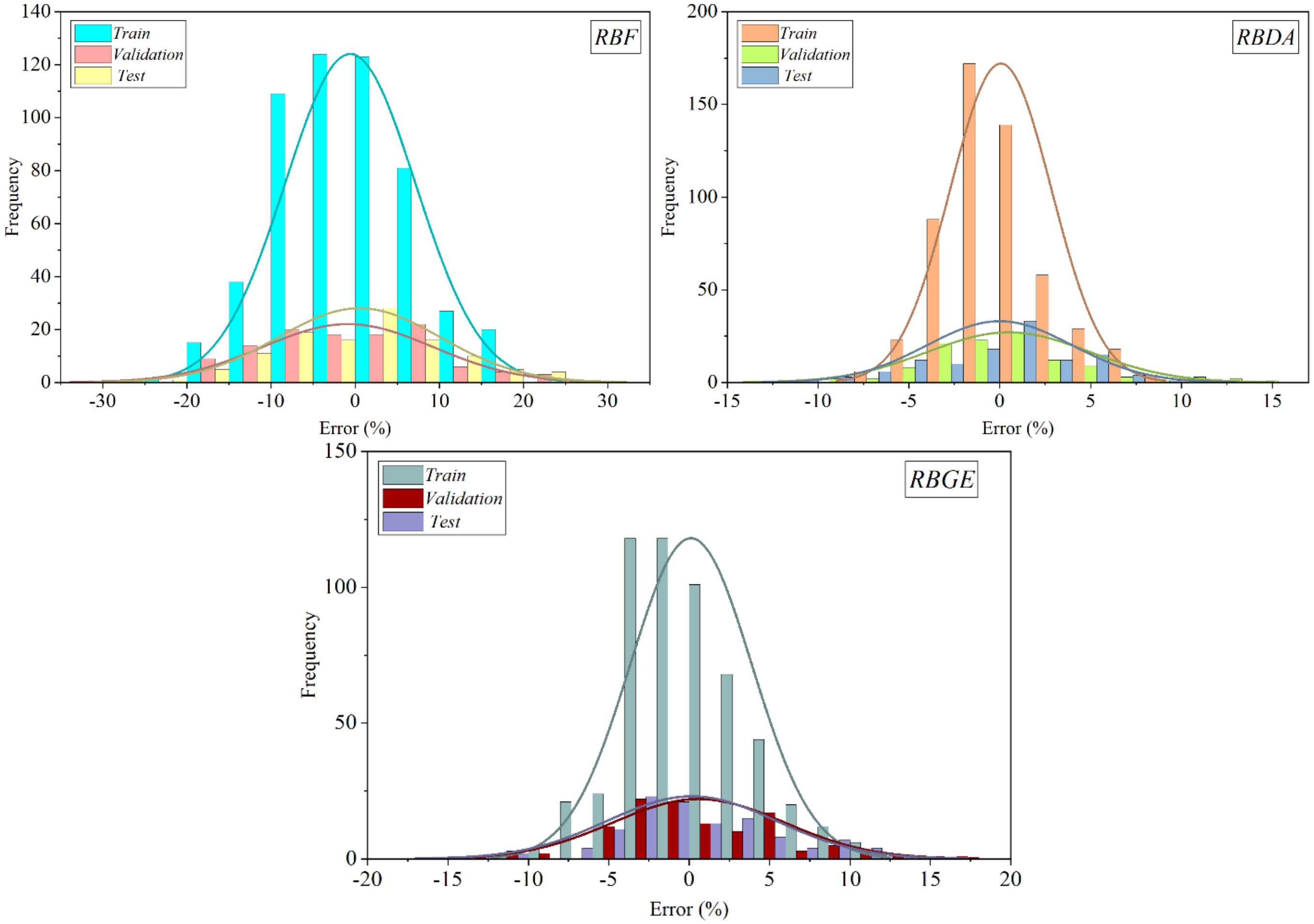

Fig. 4. The normal distribution plot serves as the foundation for the hybrid models' error percentage.

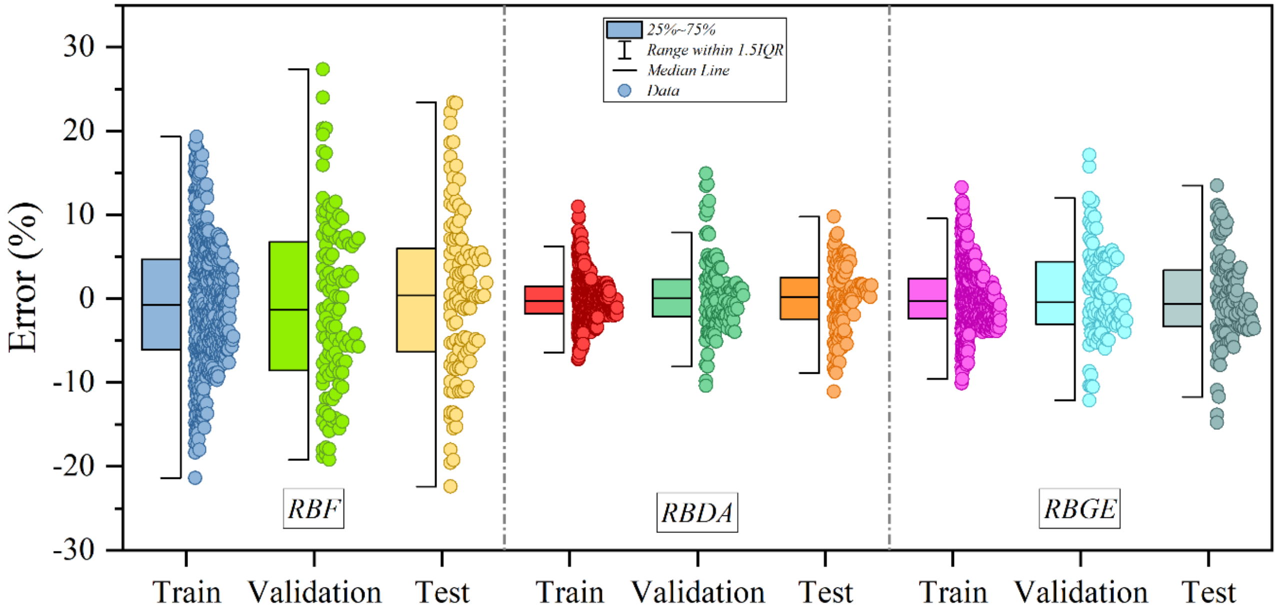

Fig. 5. The half box of errors among the developed models.

TABLE III. THE OUTCOME OF MODELS CREATED FOR RBF

| Name | Model | Results | |
|---|---|---|---|
| | | RMSE | $R^2$ |
| $Gong\ et\ al.$ [38] | $GBM$ | 0.1929 | 0.9882 |
| $Afzal\ et\ al.$ [37] | $MLP$ | 1.4122 | 0.9806 |
| $Roy\ et\ al.$ [39] | $GPR$ | 0.059 | 0.99 |
| **Present study** | **RBF+DAO** | **0.792** | **0.993** |

## IV. CONCLUSION

In conclusion, this research stressed the significance of accurate forecasting of energy use and assessment of retrofit strategies for the management of building energy systems. The weather, tenant behavior, building characteristics, and energy infrastructure all make it difficult to forecast how much energy a facility will need. Although they depend mostly on data quality and modeling complexity for accuracy, physics-based simulations may provide valuable insights. With an emphasis on Radial Basis Function (RBF) models in particular, this research examined the potential efficacy of ML techniques by using the growing amount of publicly available building energy data. Regarding the prediction of Cooling Load (CL), a significant advancement in civil engineering was made. It achieved this by effectively mitigating the constraints typically associated with ML techniques by incorporating optimization algorithms into RBF models. The forecasted outcomes generated by these models were subjected to a comparative analysis employing five distinct evaluation indices. The findings showcased the presence of a robust and exceptionally accurate predictive model, notably the RBDA (Radial Basis Function optimized with DAO), which displayed an outstanding correlation with the actual measured CL, as evidenced by a high $R^2$ value of 0.993, 1.95%, and 0.81% higher than RBF and RBGE. Additionally, it's worth noting that RBDA demonstrated the highest level of accuracy among the models, boasting a minimal RMSE value of 0.792. This represented a reduction of 47.96% compared to RBF and a 32.1% decrease compared to RBGE. Developed models solve problems and help engineers and researchers with civil engineering projects. They are reliable and precise in predicting CL, making projects safer and cheaper, and they can be helpful in future research. Addressing the limitations of this study underscores the critical importance of data quality and availability for effective ML model performance. To ensure model generalization across diverse environmental and building conditions, further validation and adaptation efforts are essential to validate broader applicability. The sensitivity of optimization algorithms to specific parameter settings necessitates meticulous fine-tuning to achieve optimal results, emphasizing the need for methodological refinement. Additionally, enriching CL predictive accuracy can be achieved by incorporating additional factors like occupant behavior dynamics or building usage patterns, enhancing practical utility in real-world scenarios. Future research should prioritize enhancing model validation through field studies to ensure robustness and reliability in varying conditions. Exploring advanced ML techniques beyond RBF models, such as deep learning architectures, can elevate prediction accuracy and unveil hidden data patterns. Dynamic model adaptation is a promising avenue for developing responsive models that adjust to evolving building dynamics and environmental factors in real time. Furthermore, integrating uncertainty analysis techniques into CL prediction models can enhance reliability by quantifying uncertainties and providing confidence intervals for predicted CL values, ultimately improving usability in practical applications.

## REFERENCES

[1] B. Sadaghat, S. Afzal, and A. J. Khiavi, “Residential building energy consumption estimation: A novel ensemble and hybrid machine learning approach,” Expert Syst Appl, vol. 251, p. 123934, 2024, doi: https://doi.org/10.1016/j.eswa.2024.123934.

[2] À. Nebot and F. Mugica, “Energy performance forecasting of residential buildings using fuzzy approaches,” Applied Sciences, vol. 10, no. 2, p. 720, 2020.

[3] J. Song, L. Zhang, G. Xue, Y. Ma, S. Gao, and Q. Jiang, “Predicting hourly heating load in a district heating system based on a hybrid CNN-LSTM model,” Energy Build, vol. 243, p. 110998, 2021.

[4] S. Ferahtia, H. Rezk, M. A. Abdelkareem, and A. G. Olabi, “Optimal techno-economic energy management strategy for building’s microgrids based bald eagle search optimization algorithm,” Appl Energy, vol. 306, p. 118069, 2022, doi: https://doi.org/10.1016/j.apenergy.2021.118069.

[5] T.-Y. Kim and S.-B. Cho, “Predicting residential energy consumption using CNN-LSTM neural networks,” Energy, vol. 182, pp. 72–81, 2019.

[6] S. Bourhnane, M. R. Abid, R. Lghoul, K. Zine-Dine, N. Elkamoun, and D. Benhaddou, “Machine learning for energy consumption prediction and scheduling in smart buildings,” SN Appl Sci, vol. 2, pp. 1–10, 2020.

[7] J. Runge and R. Zmeureanu, “Forecasting energy use in buildings using artificial neural networks: A review,” Energies (Basel), vol. 12, no. 17, p. 3254, 2019.

[8] Z. Wang, T. Hong, and M. A. Piette, “Data fusion in predicting internal heat gains for office buildings through a deep learning approach,” Appl Energy, vol. 240, pp. 386–398, 2019.

[9] J. Zhao and X. Liu, “A hybrid method of dynamic cooling and heating load forecasting for office buildings based on artificial intelligence and regression analysis,” Energy Build, vol. 174, pp. 293–308, 2018.

[10] M. Gong, Y. Bai, J. Qin, J. Wang, P. Yang, and S. Wang, “Gradient boosting machine for predicting return temperature of district heating system: A case study for residential buildings in Tianjin,” Journal of Building Engineering, vol. 27, p. 100950, 2020.

[11] S. Sarihi, F. M. Saradj, and M. Faizi, “A critical review of façade retrofit measures for minimizing heating and cooling demand in existing buildings,” Sustain Cities Soc, vol. 64, p. 102525, 2021.

[12] A. Moradzadeh, A. Mansour-Saatloo, B. Mohammadi-Ivatloo, and A. Anvari-Moghaddam, “Performance evaluation of two machine learning techniques in heating and cooling loads forecasting of residential buildings,” Applied Sciences, vol. 10, no. 11, p. 3829, 2020.

[13] L. Zhang et al., “A review of machine learning in building load prediction,” Appl Energy, vol. 285, p. 116452, 2021.

[14] Z. Wang, T. Hong, and M. A. Piette, “Building thermal load prediction through shallow machine learning and deep learning,” Appl Energy, vol. 263, p. 114683, 2020.

[15] S. S. Roy, P. Samui, I. Nagtode, H. Jain, V. Shivaramakrishnan, and B. Mohammadi-Ivatloo, “Forecasting heating and cooling loads of

buildings: A comparative performance analysis," J Ambient Intell Humaniz Comput, vol. 11, pp. 1253–1264, 2020.

[16] E. Abdelkader, A. Al-Sakkaf, and R. Ahmed, "A comprehensive comparative analysis of machine learning models for predicting heating and cooling loads," Decision Science Letters, vol. 9, no. 3, pp. 409–420, 2020.

[17] X. Li and R. Yao, "A machine-learning-based approach to predict residential annual space heating and cooling loads considering occupant behaviour," Energy, vol. 212, p. 118676, 2020, doi: https://doi.org/10.1016/j.energy.2020.118676.

[18] Y. Ding, H. Su, X. Kong, and Z. Zhang, "Ultra-short-term building cooling load prediction model based on feature set construction and ensemble machine learning," IEEE Access, vol. 8, pp. 178733–178745, 2020.

[19] Z. Xuan, Z. Xuehui, L. Liequan, F. Zubing, Y. Junwei, and P. Dongmei, "Forecasting performance comparison of two hybrid machine learning models for cooling load of a large-scale commercial building," Journal of Building Engineering, vol. 21, pp. 64–73, 2019.

[20] J. Leitao, P. Gil, B. Ribeiro, and A. Cardoso, "A survey on home energy management," IEEE Access, vol. 8, pp. 5699–5722, 2020.

[21] M. Ghalambaz, Y. R. Jalilzadeh, and A. H. Davami, "Building energy optimization using butterfly optimization algorithm," Thermal Science, vol. 26, no. 5 Part A, pp. 3975–3986, 2022.

[22] R. Wang, S. Lu, and W. Feng, "A novel improved model for building energy consumption prediction based on model integration," Appl Energy, vol. 262, p. 114561, 2020.

[23] F. E. Sapnken, M. M. Hamed, B. Soldo, and J. Gaston Tamba, "Modeling energy-efficient building loads using machine-learning algorithms for the design phase," Energy Build, vol. 283, p. 112807, Mar. 2023, doi: 10.1016/j.enbuild.2023.112807.

[24] S. Leiprecht, F. Behrens, T. Faber, and M. Finkenrath, "A comprehensive thermal load forecasting analysis based on machine learning algorithms," Energy Reports, vol. 7, pp. 319–326, 2021.

[25] A. S. Jihad and M. Tahiri, "Forecasting the heating and cooling load of residential buildings by using a learning algorithm 'gradient descent', Morocco," Case studies in thermal engineering, vol. 12, pp. 85–93, 2018.

[26] H.-J. Wang, T. Jin, H. Wang, and D. Su, "Application of IEHO–BP neural network in forecasting building cooling and heating load," Energy Reports, vol. 8, pp. 455–465, 2022.

[27] J.-S. Chou and D.-K. Bui, "Modeling heating and cooling loads by artificial intelligence for energy-efficient building design," Energy Build, vol. 82, pp. 437–446, 2014.

[28] W. Cai, X. Wen, C. Li, J. Shao, and J. Xu, "Predicting the energy consumption in buildings using the optimized support vector regression model," Energy, vol. 273, p. 127188, Jun. 2023, doi: 10.1016/j.energy.2023.127188.

[29] A. Khabthani and L. Châabane, "Development and Validation of a Cooling Load Prediction Model," International Journal of Advanced Computer Science and Applications, vol. 9, no. 2, 2018.

[30] G. I. Ahmad, J. Singla, A. Anis, A. A. Reshi, and A. A. Salameh, "Machine learning techniques for sentiment analysis of code-mixed and switched indian social media text corpus: A comprehensive review," International Journal of Advanced Computer Science and Applications, vol. 13, no. 2, 2022.

[31] G. Zhou, H. Moayedi, M. Bahiraei, and Z. Lyu, "Employing artificial bee colony and particle swarm techniques for optimizing a neural network in prediction of heating and cooling loads of residential buildings," J Clean Prod, vol. 254, p. 120082, 2020.

[32] W. Pessenlehner and A. Mahdavi, Building morphology, transparence, and energy performance. na, 2003.

[33] A. H. Alavi, A. H. Gandomi, M. Gandomi, and S. S. Sadat Hosseini, "Prediction of maximum dry density and optimum moisture content of stabilised soil using RBF neural networks," The IES Journal Part A: Civil & Structural Engineering, vol. 2, no. 2, pp. 98–106, 2009.

[34] Z. Nurlan, "A novel hybrid radial basis function method for predicting the fresh and hardened properties of self-compacting concrete," Advances in Engineering and Intelligence Systems, vol. 1, no. 01, 2022.

[35] N. Khodadadi, V. Snasel, and S. Mirjalili, "Dynamic arithmetic optimization algorithm for truss optimization under natural frequency constraints," IEEE Access, vol. 10, pp. 16188–16208, 2022.

[36] A. Mohammadi-Balani, M. D. Nayeri, A. Azar, and M. Taghizadeh-Yazdi, "Golden eagle optimizer: A nature-inspired metaheuristic algorithm," Comput Ind Eng, vol. 152, p. 107050, 2021.

[37] S. Afzal, B. M. Ziapour, A. Shokri, H. Shakibi, and B. Sobhani, "Building energy consumption prediction using multilayer perceptron neural network-assisted models; comparison of different optimization algorithms," Energy, p. 128446, Jul. 2023, doi: 10.1016/j.energy.2023.128446.

[38] M. Gong, Y. Bai, J. Qin, J. Wang, P. Yang, and S. Wang, "Gradient boosting machine for predicting return temperature of district heating system: A case study for residential buildings in Tianjin," Journal of Building Engineering, vol. 27, p. 100950, 2020.

[39] S. S. Roy, P. Samui, I. Nagtode, H. Jain, V. Shivaramakrishnan, and B. Mohammadi-Ivatloo, "Forecasting heating and cooling loads of buildings: A comparative performance analysis," J Ambient Intell Humaniz Comput, vol. 11, pp. 1253–1264, 2020.